



## Reconstruction of a magnetic flux rope from THEMIS observations

A. T. Y. Lui,<sup>1</sup> D. G. Sibeck,<sup>2</sup> T. Phan,<sup>3</sup> V. Angelopoulos,<sup>4</sup> J. McFadden,<sup>3</sup> C. Carlson,<sup>3</sup> D. Larson,<sup>3</sup> J. Bonnell,<sup>3</sup> K.-H. Glassmeier,<sup>5</sup> and S. Frey<sup>3</sup>

Received 7 December 2007; revised 10 January 2008; accepted 14 February 2008; published 16 April 2008.

[1] We investigate a magnetic flux rope (MFR) observed by THEMIS near the duskside magnetopause on 20 May 2007 using the reconstruction technique based on solving the Grad-Shafranov equation. The MFR has characteristics distinct from the adjacent magnetosheath and magnetosphere regions. In spite of these differences, the reconstruction result shows that the MFR is connected simultaneously with both the magnetosheath and the magnetosphere in terms of the magnetic vector potential characteristics. This result provides strong evidence that the MFR represents the union of these two regions. It has a small spatial dimension of  $\sim 0.5 R_E$ , a strong core magnetic field of  $>50$  nT, and an intense axial current density of  $>40$  nA/m<sup>2</sup> with non-negligible current densities transverse to its axis. **Citation:** Lui, A. T. Y., D. G. Sibeck, T. Phan, V. Angelopoulos, J. McFadden, C. Carlson, D. Larson, J. Bonnell, K.-H. Glassmeier, and S. Frey (2008), Reconstruction of a magnetic flux rope from THEMIS observations, *Geophys. Res. Lett.*, 35, L17S05, doi:10.1029/2007GL032933.

### 1. Introduction

[2] It is well recognized that the Earth's magnetosphere spans a huge volume in space. Satellites only provide point-wise in situ measurements along their paths, yielding only scanty information about the space environment. Naturally, it is highly desirable to have several spacecraft available and to develop tools that allow one to extract 3D information from such multi-spacecraft observations [e.g., *Glassmeier et al.*, 2001; *Dunlop et al.*, 2002]. When this is not impossible, analysis tools are required that may enable extended vision of space environment from single point measurements. Such a useful tool called Grad-Shafranov reconstruction has been developed by Bengt Sonnerup and his colleagues to examine magnetic flux ropes near the magnetopause, in the solar wind, and in the magnetotail (see *Sonnerup et al.* [2006] for an overview). The technique is initially employed to analyze data from a single satellite [*Sonnerup and Guo*, 1996; *Hau and Sonnerup*, 1999; *Hu and Sonnerup*, 2001, 2003; *Teh and Hau*, 2004, 2007] and is now extended to treat measurements from multiple satellites [*Sonnerup et al.*, 2004; *Hasegawa et al.*, 2005, 2006, 2007]. The assumptions in employing this technique were listed by *Hau and Sonnerup* [1999], with additional caveats given by

*Hasegawa et al.* [2007] based on tests with simulation data.

[3] In this paper, we show the reconstruction of a magnetic flux rope adjacent to the magnetopause detected by the recently launched THEMIS (Time History of Events and Macroscopic Interactions during Substorms) mission [*Angelopoulos*, 2008]. Salient features of this structure, which cannot be directly measured by a single satellite, are extracted with the Grad-Shafranov reconstruction. The results provide strong evidence that this plasma structure has connection to both the magnetosheath and the magnetosphere. The spatial dimension of the structure is small,  $\sim 0.5 R_E$ . Its embedded core magnetic field is high at  $>50$  nT, accompanied by a strong axial current density with a peak at  $>40$  nA/m<sup>2</sup> and non-negligible transverse current densities.

### 2. Benchmarking of the GS Solver

#### 2.1. Background

[4] As discussed by *Sonnerup et al.* [2006], reconstruction of plasma configuration from observation by a single satellite is based on solving the Grad-Shafranov (GS) equation assuming the structure to have a two-dimensional (2D) MHD equilibrium. The equation is

$$\left(\frac{\partial^2}{\partial x^2} + \frac{\partial^2}{\partial y^2}\right)A = -\mu_0 \frac{dP_t(A)}{dA},$$

where the transverse pressure is given by  $P_t = p + B_z^2/2\mu_0$  ( $p$  is the plasma pressure). The magnetic field vector  $\mathbf{B}$  is related to the partial vector potential  $A(x, y)$  and the axial magnetic field  $B_z$  by  $\mathbf{B} = \nabla A(x, y) \times \hat{z} + B_z(A)\hat{z}$ . The third dimension represents the direction along which the structure changes much more gradually in comparison to the variation on the plane perpendicular to it. The GS equation is solved as a spatial initial value problem. We have adopted the procedure documented by *Hau and Sonnerup* [1999] in this work.

#### 2.2. Benchmark With a Theoretical Model and IRM Data

[5] For benchmarking of the GS solver we have developed, we check out the code with the two test cases given by *Hau and Sonnerup* [1999]. The first one is a theoretical model in which the partial magnetic vector potential is given by

$$A(x, y) = \ln\left\{\alpha \cos(x) + \sqrt{1 + \alpha^2} \cosh(y)\right\},$$

where  $\alpha = 0.225$ , the plasma pressure by  $p = e^{-2A}/(3\mu_0)$ , and the axial magnetic field by  $B_z = e^{-A}/\sqrt{3}$ . For testing, the

<sup>1</sup>JHU APL, Laurel, Maryland, USA.

<sup>2</sup>NASA GSFC, Greenbelt, Maryland, USA.

<sup>3</sup>Space Sciences Laboratory, University of California, Berkeley, California, USA.

<sup>4</sup>IGPP, University of California, Los Angeles, California, USA.

<sup>5</sup>IGEP, Technische Universität, Braunschweig, Germany.

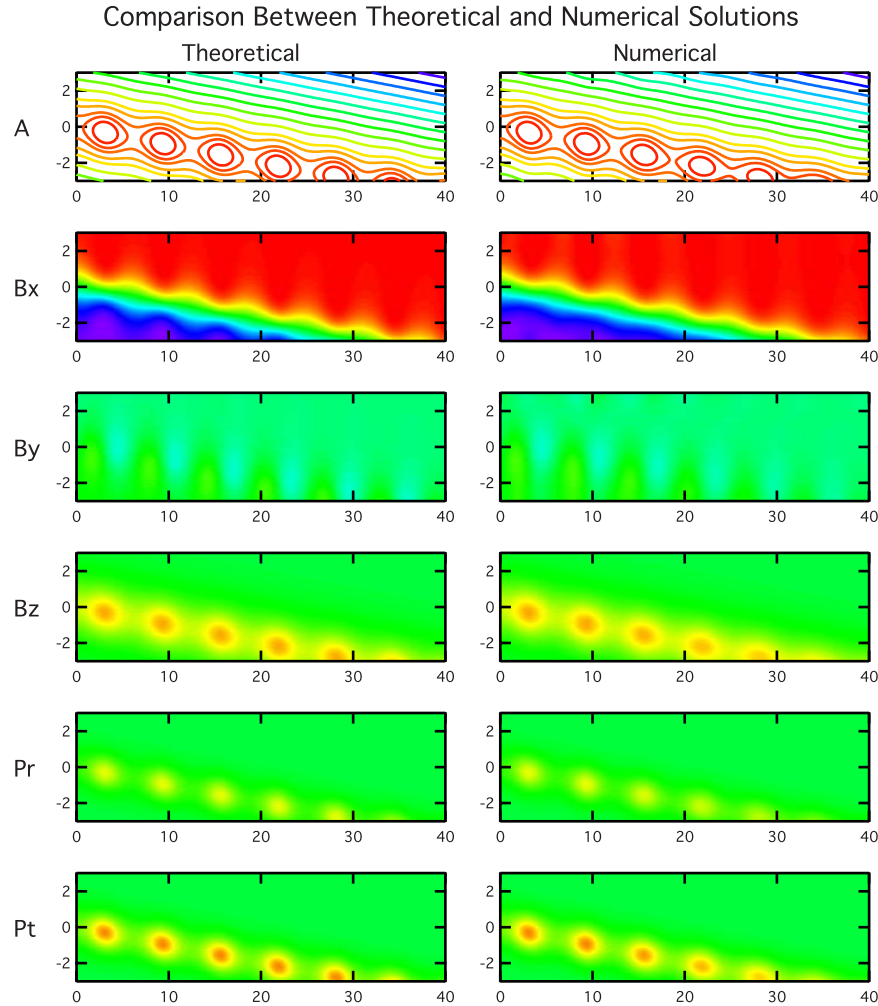


**Figure 1.** Benchmarking of the GS solver with a theoretical model: comparison of six plasma parameters between the (left) theoretical and (right) numerical solutions.

model structure is rotated by  $5.7^\circ$  with respect to the satellite path, as done by *Hau and Sonnerup* [1999]. The theoretical (left column) and the numerical (right column) solutions for the six parameters are given in Figure 1, showing very good match of the numerical solutions with the theoretical ones. Small differences may be noticed at the upper and lower edges of these panels. The error in the numerical solution of  $A(x, y)$  in the entire map ranges from  $-5.3\%$  to  $6.0\%$ . The second example is the IRM event on October 19, 1984, 0517:41–0519:48 UT. The results obtained by our GS solver also resemble closely with those shown in Figure 6 of *Hau and Sonnerup* [1999].

### 3. THEMIS Observations and GS Reconstruction

#### 3.1. Magnetic Flux Rope Detection

[6] A magnetic flux rope was detected by the THEMIS satellites on May 20, 2007 (D. G. Sibeck et al., Crater FTEs: Simulation results and THEMIS observations, submitted to *Geophysical Research Letters*, 2008). Figure 2 shows the plasma and magnetic field measurements obtained by the electrostatic analyzer [*Carlson et al.*, 2008] and the flux-gate magnetometer [*Auster et al.*, 2008], respectively, on THEMIS D during this interval with the satellite location

given at the bottom. The GSE coordinate system is used throughout this work unless stated otherwise. The satellite was in the magnetosheath at the start of the interval, indicated by the high plasma density, a relatively steady tailward plasma flow of  $\sim 150$ – $200$  km/s, and fluctuating southward magnetic field. At  $\sim 2157$  UT, it entered the magnetosphere with a low plasma density, much reduced tailward plasma flow, and a distinctly different magnetic field orientation and magnitude. This entry lasted for only  $\sim 2$  min as it re-entered the magnetosheath. In the next  $\sim 5$  min ( $\sim 2159$ – $2204$  UT), the plasma density was high again. Within this time interval, there was a prominent feature with high magnetic field strength accompanied by a somewhat reduced tailward plasma flow of  $\sim 100$  km/s. This feature is shown in Figure 2 between the vertical dashed lines. The magnetic field components were distinct from those in the magnetosheath and the magnetosphere. The  $B_x$  and  $B_y$  components had a bipolar signature. These characteristics suggest the encounter of a magnetic flux rope (MFR).

#### 3.2. Analysis and Transformation

[7] The first step in the GS reconstruction is to examine the structure with the minimum variance analysis (MVA)

2007 May 20 THEMIS-D/ESA/FGM

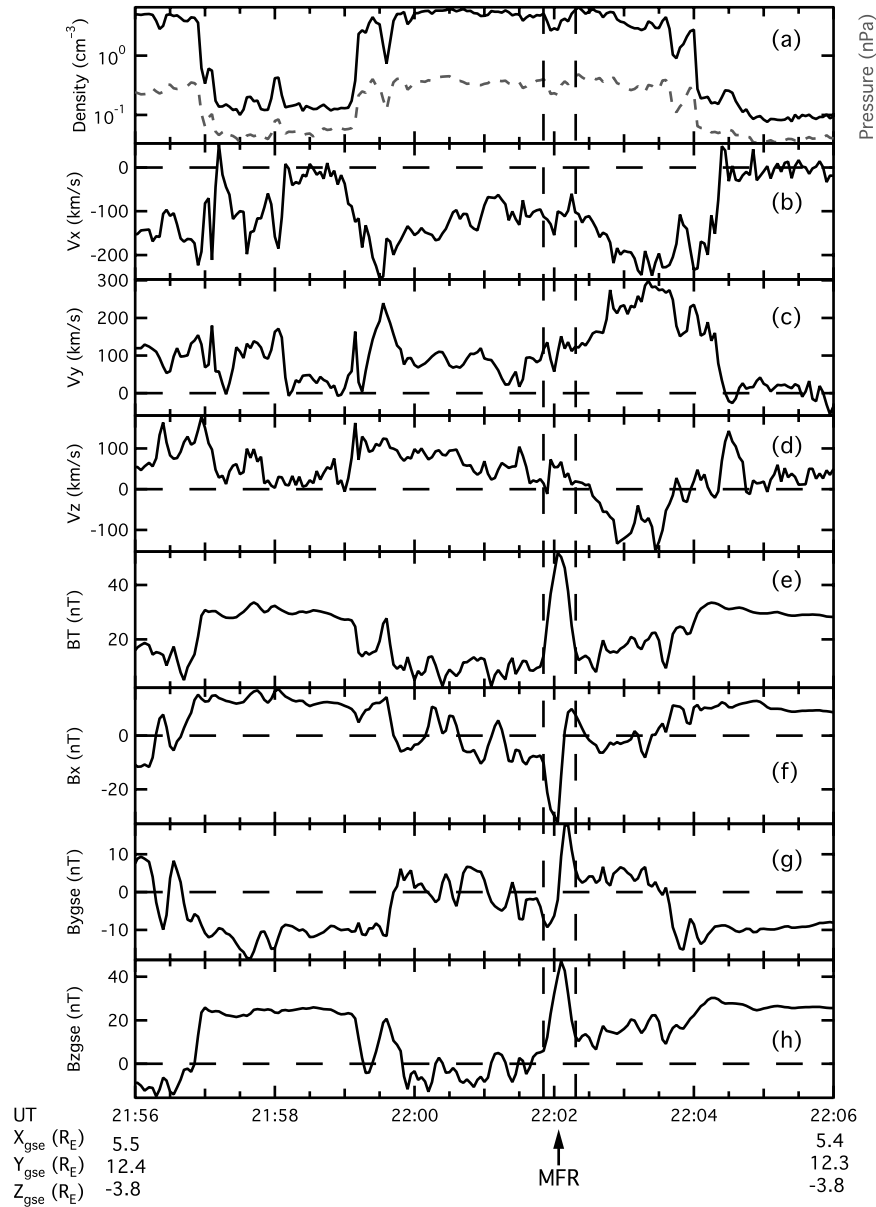


**Figure 2.** Plasma parameters near the dusk magnetopause measured by THEMIS D: (a) the number density is given by the solid line and the pressure is given by the dashed line; also shown are (b–d) the three components of the plasma bulk flow and (e–h) the total magnitude and the three components of the magnetic field.

and with the deHoffman-Teller (HT) transformation for the appropriateness of the steady-state equilibrium assumption. The hodograms from MVA are shown in Figure 3a for the interval 2201:50–2202:20 UT. The coordinates of these axes are  $B_N = (-0.2065, -0.2497, 0.9461)$ ,  $B_M = (-0.8677, -0.4936, -0.0592)$ , and  $B_L = (-0.4522, 0.8331, -0.3186)$ , with the eigenvalues of 4.364, 177.1, and 243.1, respectively. The MVA result indicates a well-defined  $B_N$  axis, conforming well to a 2D structure.

[8] Figure 3b shows the results of the HT transformation for the interval 2201:30–2202:30 UT. The deHoffman-Teller velocity  $V_{\text{HT}}$  is found to be  $(-91.8, 123.6, -33.6)$  km/s. The correlation coefficient between  $-(V \times B)_y$  and

$-(V_{\text{HT}} \times B)_y$  is 0.969, indicating the existence of a moving frame in which the structure fits well with a relatively steady state condition. The small slope for  $V - V_{\text{HT}}$  versus  $V_a$  (Alfvén velocity) shows the lack of fast flows in the transformed frame, again consistent with the steady state assumption for the structure. These results show that the observed structure has properties satisfying the assumptions for the GS reconstruction.

### 3.3. Reconstruction Results

[9] Following the procedure documented by *Hau and Sonnerup* [1999] to find an appropriate frame for GS reconstruction, we rotate by an angle  $\theta$  the  $B_M$  axis about

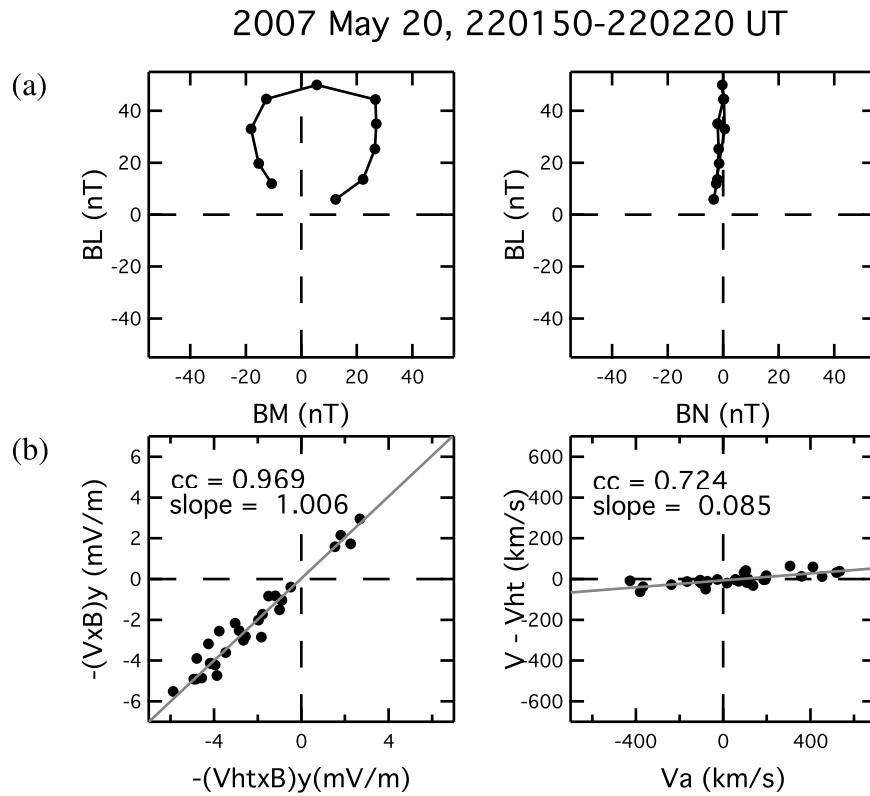


**Figure 3.** (a) Results from minimum variance analysis and (b) results from HT frame transformation.

the  $B_N$  axis to form a new  $Z$ -axis and then assign the new  $Y$ -axis to be  $B_N$  and the new  $X$ -axis to be  $V_{HT}$  projected on the new  $XY$ -plane. The angle  $\theta$  is chosen by trial and error to obtain a simple dependence of  $P_t$  and  $B_z$  on  $A(x, y)$ . These parameters are fitted by a combination of polynomial and exponential functions of  $A(x, y)$ . This exercise gives  $\theta = -75^\circ$ . The resulting new axes are  $X = (0.5268, -0.7761, 0.3466)$ ,  $Y = (0.7366, 0.6203, 0.2694)$ , and  $Z = (-0.4241, 0.1134, 0.8985)$  in GSE coordinates.

[10] Figure 4a shows the variation of  $A(x, y)$  along the satellite path and the dependence of  $P_t$  on  $A(x, y)$  including its fitting curve. The normalization for  $A(x, y)$  is 0.19 T-m. It is evident that  $P_t$  assumes double values in the range of 0–0.5 for  $A(x, y)$ . Although not shown, similar double-value dependence is found for  $B_z$ . If the structure were associated with only one region, then no double-value dependence would exist. The existence of the double-value dependence indicates that part of the structure belongs to one branch of  $A(x, y)$  (magnetosheath branch) while the other part belongs to a different branch of  $A(x, y)$  (magnetosphere branch), testifying that this structure represents the union of these two plasma regions.

[11] The profiles of  $p$  and  $B_z$  along the satellite path are shown in Figure 4b. The appreciable drop in  $p$  is accompanied by a substantial increase in  $B_z$ , consistent with the trend for total pressure balance across the structure. The comparison between the observed and model values for magnetic field components is given in Figure 4c. The correlation coefficient is 0.9978, indicating that the agreements between these quantities are extremely good.

### 3.4. Reconstruction Maps

[12] The usefulness in the GS reconstruction lies in the extension of the measurements along the satellite path in a direction perpendicular to its path, producing a 2D map of plasma parameters. Such 2D maps for the partial vector potential, magnetic field components, plasma pressure, and current densities are shown in Figure 5. The current density is derived from  $\text{curl } \mathbf{B}$  using the same 2D approximation adopted for the GS reconstruction. The magnetic flux rope has a small spatial dimension of  $\sim 0.5 R_E$ . The current density maps show the axial current density to be quite high, in excess of 40 nA/m<sup>2</sup>. Furthermore, the current density components on this  $XY$ -plane are not negligible either. The axial magnetic field is also quite high, in excess of 50 nT, and is associated with a low plasma pressure.

## 4. Summary and Discussion

[13] We have developed and benchmarked the software to perform the Grad-Shafranov reconstruction [Sonnerup *et al.*, 2006, and references therein]. Based on observations from a THEMIS satellite on 20 May 2007, we have successfully reconstructed the configuration of a magnetic flux rope surrounding the satellite path. This magnetic flux rope has characteristics distinct from those in the adjacent regions of the magnetosphere and the magnetosheath. The spatial dimension of this structure is small,  $\sim 0.5 R_E$ . The core magnetic field is high,  $>50$  nT. The structure appears to be in static equilibrium, being convected downstream at a speed of  $\sim 100$  km/s.

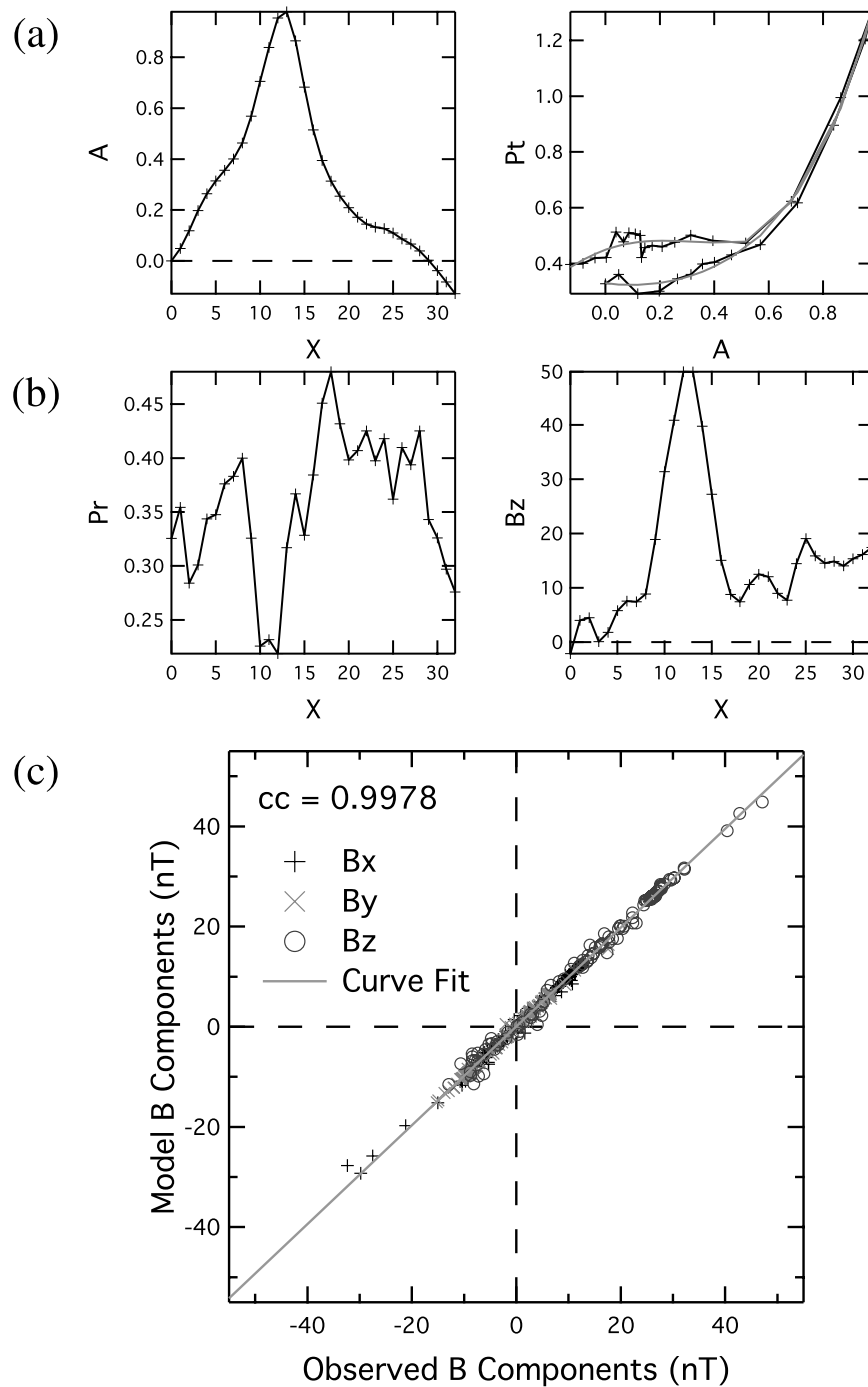


**Figure 4.** (a) The partial vector potential  $A(x, y)$  as a function of the satellite path ( $X$ ) and the transverse pressure ( $P_t$ ) as a function of  $A(x, y)$ , (b) the plasma pressure ( $Pr$ ) and axial magnetic field ( $B_z$ ) as a function of  $X$ , and (c) comparison of magnetic field components between observed and model values.

[14] From the properties of magnetic vector potential obtained through the reconstruction, it is found that the magnetic flux rope has one part connected with the magnetosheath and another part connected with the magnetosphere. *Hu and Sonnerup* [2003] have used different branches for magnetosheath and magnetosphere in their reconstruction of an extended interval that spans over these two regions. They have identified a central current layer at the magnetopause containing interconnected magnetic field

lines but no magnetic flux rope with a strong core field was evident in the data. *Hasegawa et al.* [2006] have examined five flux transfer events from Cluster observations. They have used different branches of the partial vector potential in combining different Cluster measurements for reconstruction. The result reported here shows for the first time that different branches of the partial magnetic vector potential are obtained for a magnetic flux rope from reconstruction of measurements from a single satellite, constituting

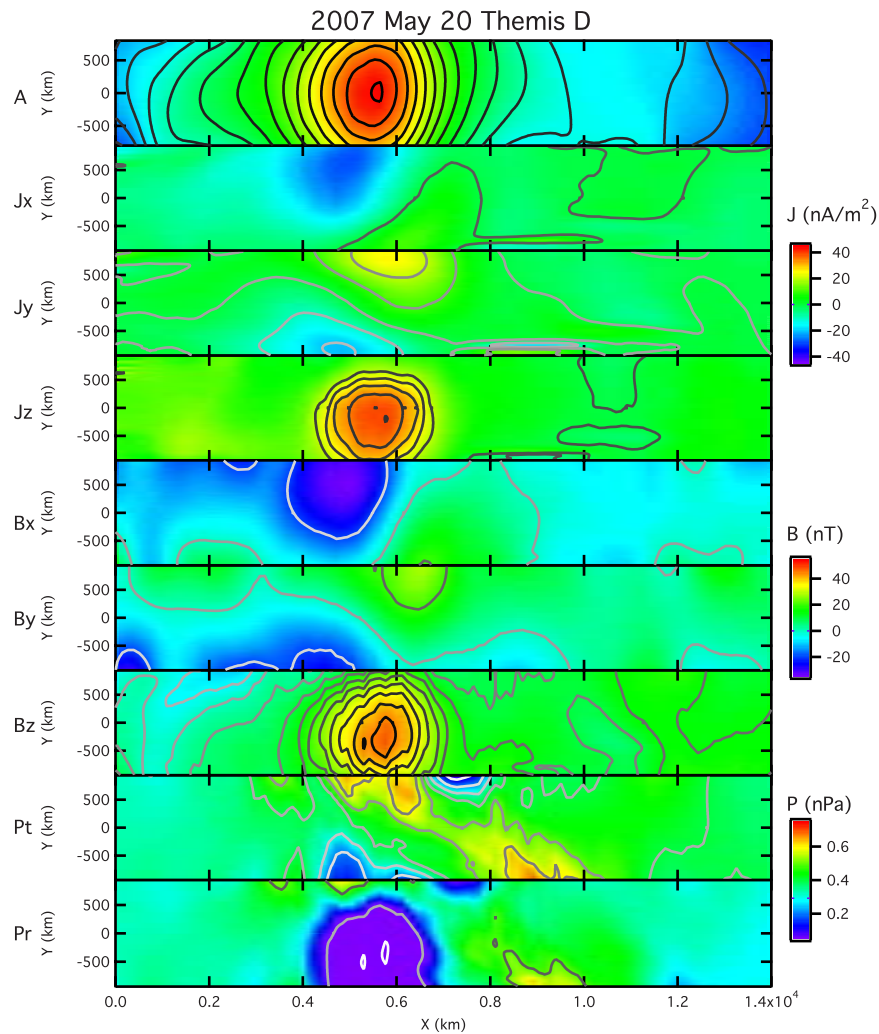


**Figure 5.** 2D maps of partial magnetic vector potential, current density components, magnetic field components, transverse pressure, and plasma pressure obtained from the reconstruction.

convincing evidence that the plasma structure observed near the magnetopause is a union of the two regions.

[15] The fact that the magnetic flux rope is a union of two regions is consistent with the expected properties of a flux transfer event [Russell and Elphic, 1978; Lee and Fu, 1985]. The presence of a strong core field in the flux transfer event supports the earlier result of Hasegawa *et al.* [2006] that it indicates component merging. Since the core magnetic field is larger than the field component seen in the magnetosheath and the magnetopause, this flux transfer event is consistent with the model proposed by Lee and Fu [1985] in which multiple reconnection sites are needed to generate the intense core field.

[16] One important result from this study is that the surrounding current density components associated with the flux transfer event are shown to be quite significant, even on the plane perpendicular to its axis.

[17] Overall, we have independently confirmed many results from Grad-Shafranov reconstruction published by Bengt Sonnerup and his colleagues. Combining observations from all THEMIS satellites to produce a composite 2D

reconstruction map of this magnetic flux rope will be reported in the future.

[18] **Acknowledgments.** This work was supported by the NASA contract NAS5-02099 to University of California, Berkeley, by the NSF grant ATM-0630912 and NASA grant NNX07AU74G to the Johns Hopkins University Applied Physics Laboratory, and by the German Ministerium für Wirtschaft und Technologie and the Deutsches Zentrum für Luft- und Raumfahrt under grant 50QP0402 to the FGM Lead Investigator Team at the Technical University of Braunschweig.

## References

- Angelopoulos, V. (2008), The THEMIS mission, *Space Sci. Rev.*, in press.
- Auster, H. U., et al. (2008), The THEMIS fluxgate magnetometer, *Space Sci. Rev.*, in press.
- Carlson, C. W., et al. (2008), The THEMIS ESA plasma instrument and in-flight calibration, *Space Sci. Rev.*, in press.
- Dunlop, M. W., A. Balogh, K.-H. Glassmeier, and P. Robert (2002), Four-point Cluster application of magnetic field analysis tools: The Curlometer, *J. Geophys. Res.*, *107*(A11), 1384, doi:10.1029/2001JA005088.
- Glassmeier, K.-H., et al. (2001), Cluster as a wave telescope—First results from the fluxgate magnetometer, *Ann. Geophys.*, *19*, 1439–1447.
- Hasegawa, H., et al. (2005), Optimal reconstruction of magnetopause structures from Cluster data, *Ann. Geophys.*, *23*, 973–982.
- Hasegawa, H., et al. (2006), The structure of flux transfer events recovered from Cluster data, *Ann. Geophys.*, *24*, 603–618.

- Hasegawa, H., R. Nakamura, M. Fujimoto, V. A. Sergeev, E. A. Lucek, H. Rème, and Y. Khotyaintsev (2007), Reconstruction of a bipolar magnetic signature in an earthward jet in the tail: Flux rope or 3-D guide-field reconnection?, *J. Geophys. Res.*, *112*, A11206, doi:10.1029/2007JA012492.
- Hau, L.-N., and B. U. Ö. Sonnerup (1999), Two-dimensional coherent structures in the magnetopause: Recovery of static equilibria from single-spacecraft data, *J. Geophys. Res.*, *104*, 6899–6917.
- Hu, Q., and B. U. Ö. Sonnerup (2001), Reconstruction of magnetic flux ropes in the solar wind, *Geophys. Res. Lett.*, *28*, 467–470.
- Hu, Q., and B. U. Ö. Sonnerup (2003), Reconstruction of two-dimensional structures in the magnetopause: Method improvements, *J. Geophys. Res.*, *108*(A1), 1011, doi:10.1029/2002JA009323.
- Lee, L. C., and Z. F. Fu (1985), A theory of magnetic flux transfer at the Earth's magnetopause, *Geophys. Res. Lett.*, *12*, 105–108.
- Russell, C. T., and R. C. Elphic (1978), Initial ISEE magnetometer results - Magnetopause observations, *Space Sci. Rev.*, *22*, 681–715.
- Sonnerup, B. U. Ö., and M. Guo (1996), Magnetopause transects, *Geophys. Res. Lett.*, *23*, 3679–3682.
- Sonnerup, B. U. Ö., H. Hasegawa, and G. Paschmann (2004), Anatomy of a flux transfer event seen by Cluster, *Geophys. Res. Lett.*, *31*, L11803, doi:10.1029/2004GL020134.
- Sonnerup, B. U. Ö., H. Hasegawa, W.-L. Teh, and L.-N. Hau (2006), Grad-Shafranov reconstruction: An overview, *J. Geophys. Res.*, *111*, A09204, doi:10.1029/2006JA011717.
- Teh, W.-L., and L.-N. Hau (2004), Evidence for pearl-like magnetic island structures at dawn and dusk side magnetopause, *Earth Planets Space*, *56*, 681–686.
- Teh, W.-L., and L.-N. Hau (2007), Triple crossings of a string of magnetic islands at duskside magnetopause encountered by AMPTE/IRM satellite on 8 August 1985, *J. Geophys. Res.*, *112*, A08207, doi:10.1029/2007JA012294.
- 
- V. Angelopoulos, IGPP, UCLA, Los Angeles, CA 90095-1567, USA.  
K.-H. Glassmeier, IGEP, TU, D-38106 Braunschweig, Germany.  
J. Bonnell, C. Carlson, S. Frey, D. Larson, J. McFadden, and T. Phan, Space Sciences Laboratory, University of California, Berkeley, CA 94720, USA.  
A. T. Y. Lui, JHU APL, Laurel, MD 20723-6099, USA. (tony.lui@jhuapl.edu)  
D. G. Sibeck, NASA GSFC, Greenbelt, MD 20771, USA.